Feature Reliability and Uncertainty-Aware Fuzzy Learning for COVID-19 Lesion Segmentation

[1]Dhiraj Kumar Raut, [2]Arla Gopala Krishna, [3]Sowkuntla Pandu*

[1, 2, 3]Department of Computer Science and Engineering, SRM University, Amaravati, 522502, Andhra Pradesh, India
[1]dhiraj_kumarraut@srmap.edu.in
[2]gopalakrishna_arla@srmap.edu.in
[3]pandu.edu@gmail.com

Abstract. There is still the difficult task of accurate delineation of the COVID-19 infection regions in the CT-based scan of the chest, since the lesions have blurred edges, the contrast between infected and noninfected tissues is low, and the lesion appearance is highly variable. Though encoder-decoder-based architectures like U-Net and its variations have been shown to perform well, they are generally not capable of coping with uncertainty and noise around lesion edges, producing segmentation output in fragments or with errors. In order to solve these issues, we introduce AFR-Net, an adaptive fuzzy reasoning segmentation network that explicitly represents feature reliability and boundary uncertainty in a single deep learning model. The given approach is developed by the fuzzy feature reliability module that is aimed at estimating the reliability of encoder features based on the fuzzy inference rules, so that unreliable or noisy features can be blocked during feature fusion. Moreover, the decoder has a fuzzy boundary consistency module that further refines the lesion boundaries based on the reasoning of the local gradient variations and regional homogeneity. All of these fuzzy reasoning elements cooperate to steer the segmentation process, enabling the network to capture the ambiguous regions more appropriately and come up with more consistent lesion boundaries. The proposed framework is evaluated on the MosMedData COVID-19 CT dataset, which contains 1110 chest CT scans with pixel-level infection annotations, and compared with competitive baseline models, including U-Net, U-Net++, and ResUNet. The results of the experiment demonstrate that AFR-Net has more precise and consistent segmentation performance, indicating its efficiency as an interpretable and uncertainty-sensitive model to segment COVID-19 lesions.

Keywords: COVID-19 lesion segmentation, fuzzy reasoning, medical image segmentation, U-Net, uncertainty modelling.

1 Introduction

As reported, the global spread of COVID-19 has emerged as a significant challenge to the healthcare systems throughout the world, which highlights the importance of precise and effective diagnostic and assessment instruments. Chest computed tomography (CT) imaging has become a popular and significant supplementary modality to assess

B. Singh et al. (eds.), *Proceedings of the International Conference on Advances in Computing Technology and Artificial Intelligence (COMPUTATIA 2026)*, Atlantis Highlights in Intelligent Systems 18,
https://doi.org/10.2991/978-94-6239-713-2_8

COVID-19 infections, as it offers a detailed view of lung abnormalities, including ground-glass opacities and consolidations [1, 2]. Quantitative disease assessment, treatment planning, and monitoring of disease progression require the precise segmentation of lesion regions of the CT images to assess the disease. COVID-19 lesion segmentation is a complicated issue, even in spite of its significance, because of the nature of lung CT images. The areas of infection tend to have blurred and irregular borders and decreased contrast to the adjacent healthy tissue, as well as extensive size and shape variations in their appearance [3]. Moreover, the imaging noise, partial volume effect, and inter-patient variability increase the uncertainty of the lesion appearance, and thus, it becomes particularly challenging to ensure reliable automated segmentation. The last few years have seen the use of deep learning-based encoder-decoder architectures, which are now the popular method of segmenting medical images. One of them is the popular U-Net because of its symmetric design and an efficient application of skip connections to merge features together [4, 5]. A number of variations of the U-Net have been suggested to improve the results of segmentation. U-Net++ and ResUNet adopt nested and dense skip connections to enhance multi-scale feature aggregation and residual learning to encourage gradient propagation and more profound feature extraction, respectively. These models have demonstrated strong performance across multiple medical image segmentation tasks, including COVID-19 CT infection segmentation. Despite these architectures achieving encouraging performances, they are usually based on deterministic feature extraction and fusion processes [6]. Consequently, any feature detected in an ambiguous or noisy area is commonly given equal consideration as the good features, and this may result in a poor prediction in the area surrounding the lesion. It is a limitation that is especially important with COVID-19 CT images, where the boundary ambiguity and intensity overlap between infected and healthy tissues are prevalent in these images [7].

To overcome these limitations, this paper proposes AFR-Net, an adaptive fuzzy-reasoning-based segmentation system for COVID-19 lesion segmentation on the chest CT images. Rather than stochastically mapping the uncertainty directly into the convolutional operations, the proposed approach entails the notion of fuzzy rationale at the levels of the reliability of the features and the refinement of the boundaries. This structure enables the uncertainty processing to be separate from core feature extractors, maintaining the strengths of conventional encoder-decoder designs and enjoying the benefits of interpretable fuzzy inference. The proposed framework is based on a typical encoder-decoder backbone and incorporates two important elements that are motivated by fuzzy logic. A fuzzy feature reliability module is proposed to determine the reliability of encoder features by relying on cues associated with uncertainty, and the unreliable information can be suppressed adaptively during the fusion of the features. Moreover, a fuzzy boundary consistency module further refines the outputs of segmentation using reasoning on the local gradient changes and local homogeneity and comes up with smoother and more precise lesion boundaries. The key contributions of this work are outlined by

1. We propose an adaptive fuzzy reasoning–based segmentation framework for COVID-19 lesion segmentation that explicitly addresses feature uncertainty and boundary ambiguity.

2. We introduce a fuzzy feature reliability module that evaluates the trustworthiness of encoder features using interpretable fuzzy inference rules.
3. We design a fuzzy boundary consistency module to refine lesion boundaries by reasoning over local gradient and regional homogeneity information.
4. The rest of this paper is structured in the following way. Section 2 outlines the related work in existence, and Section 3 outlines the AFR-Net, an adaptive fuzzy reasoning-based segmentation framework, in detail. The experimental setup and results are presented in Section 4, offering a comparative study with baseline models. Last but not least, Section 5 concludes the paper and describes the possible way of future work.

2. Related Work

2.1 Deep Learning for Medical Image and COVID-19 Lesion Segmentation

Deep neural networks are the dominant approach for segmentation tasks of medical images because they can learn complex patterns directly from data. Encoder–decoder architectures have been particularly effective, as they combine high-level semantic features with detailed spatial information. Among them, U-Net remains one of the most widely used models because of its symmetric structure and skip connections that enable accurate localization [4]. Consequently, U-Net is commonly adopted as a baseline for lung and lesion segmentation tasks. Many improved versions of U-Net have been developed to enhance feature fusion and segmentation performance. U-Net++ introduces nested and dense skip connections to reduce the semantic gap between encoder and decoder features [5], while ResUNet incorporates residual learning to facilitate deeper networks and more stable training [8]. Attention U-Net enhances segmentation by emphasizing relevant spatial regions through attention gates [9], and U-Net 3+ aggregates multi-scale features using full-scale skip connections to improve performance across different resolutions [10]. Despite these improvements, most of these models rely on deterministic feature extraction and fixed fusion strategies. With the outbreak of COVID-19, mostly the methods rely on deep neural networks. Techniques have been extensively explored for precise infection region segmentation of chest CT images. Early studies demonstrated the effectiveness of convolutional networks in identifying lung infections and supporting quantitative analysis [3]. Inf-Net introduced a specialized architecture with edge guidance to improve COVID-19 lesion segmentation [11], while other works focused on lightweight and efficient models for rapid diagnosis and analysis [7, 12]. Nevertheless, COVID-19 lesion segmentation remains challenging due to blurred boundaries, heterogeneous lesion appearance, and intensity overlap with healthy tissues, motivating the need for more uncertainty-aware segmentation strategies.

2.2 Uncertainty Modeling in Medical Image Segmentation

Uncertainty-aware learning has gained more popularity in medical image studies, as it provides insights into prediction reliability and improves robustness in ambiguous regions. Bayesian neural networks and Monte Carlo dropout have been widely explored to estimate model uncertainty by performing stochastic inference [13]. Kendall and Gal further distinguished between epistemic and aleatoric uncertainty and demonstrated their importance in deep learning–based vision tasks [14]. Medical image segmentation has also been done using ensemble-based methods to enhance reliability and generalization [15]. Though they are effective methods of uncertainty modeling, such models tend to demand several forward passes or numerous models, which makes them more expensive and less efficient. Further, these probabilistic methods can be uninterpretable, and it can be hard to determine the role of uncertainty in decision-making on segmentation, especially in clinical practices.

2.3 Fuzzy Logic for Handling Uncertainty in Medical Imaging

Fuzzy logic offers a natural and understandable system of representing uncertainty, imprecision, and vagueness that are inherent traits of medical images. Classical fuzzy systems have found application in image segmentation, wherein membership functions and rule-based reasoning are used to deal with the ambiguous boundaries and the noisy information [16]. With the rise of deep learning, fuzzy logic has increasingly been integrated with neural networks to enhance robustness and interpretability in medical image analysis [6]. Several fuzzy deep learning approaches embed fuzzy operations directly into convolutional layers or attention mechanisms, aiming to improve feature representation in uncertain regions. While such methods can enhance segmentation accuracy, they often introduce additional architectural complexity and computational overhead. Furthermore, tightly coupling fuzzy logic with low-level convolutional operations may reduce flexibility and make the models harder to adapt to different datasets or clinical scenarios [14, 16].

3. Proposed Method

This section describes the suggested AFR-Net, an adaptive fuzzy reasoning-based framework designed for accurate and uncertainty-aware segmentation of infected regions of COVID-19. The proposed framework consists of three main components: (1) hierarchical feature extraction using a standard encoder-decoder architecture, (2) a fuzzy feature reliability module to assess the trustworthiness

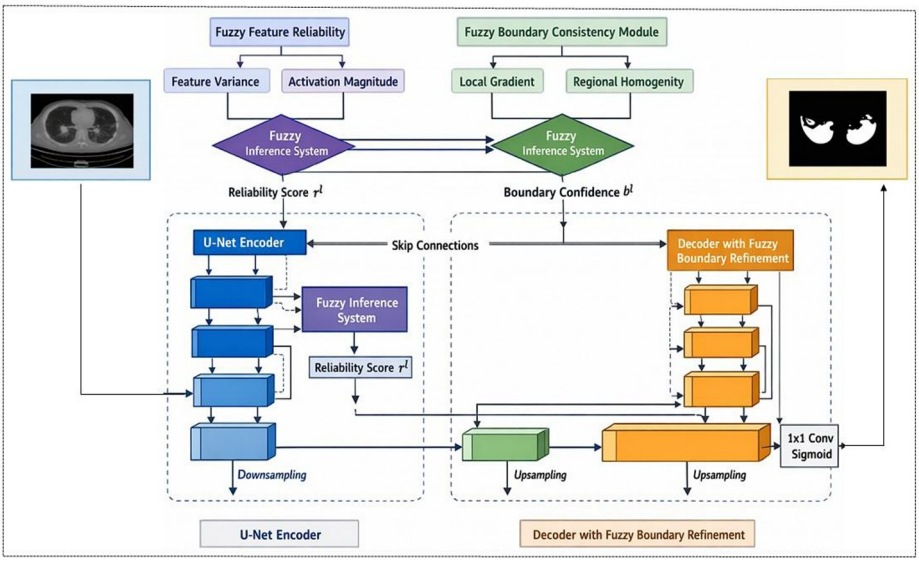

Fig. 1: Architecture of the proposed AFR-Net with fuzzy feature reliability and boundary refinement

The proposed framework consists of an encoder module, a decoder module that processes the encoder features, and a fuzzy boundary consistency module to refine lesion boundaries during decoding. An overall flow of the proposed framework is illustrated conceptually in Fig. 1.

3.1 Encoder-Decoder-Based Hierarchical Feature Extraction

AFR-Net adopts a standard encoder–decoder architecture as its backbone because this structure has demonstrated better improvements in the sector of medical image segmentation tasks. Both the encoder and decoder sequentially retrieve the hierarchical feature representations with convolution and downsampling, respectively, and upsampling and feature fusion restore spatial resolution, respectively. The encoder and decoder features of different scales are combined by means of skip connections to be able to preserve the spatial details. In contrast to conventional versions of U-Net, which simply combine encoder features without paying attention to their accuracy, AFR-Net presents fuzzy reasoning units, which steer feature integration and boundary optimization. Fuzzy logic is also used in higher-level decisions, which means that instead of involving convolutional operations, it is used in situations where there is a need to handle uncertainty, which can be decoupled from the fundamental feature extraction.

3.2 Encoder-Decoder-Based Hierarchical Feature Extraction

The features that have been extracted from medical images might be characterized by varying levels of uncertainty, especially in those areas that are encircled by noise, low contrast, or even blurred lesion boundaries. To solve this problem, we come up with a

fuzzy feature reliability module, which is used to gauge the credibility of encoder features prior to blending them with features of the decoder. Let F_e^l represent the feature output of the encoder extracted at level l. . Two feature-related cues are derived based on F_e^l: feature variance vl and activation magnitude ml. Local inconsistency is represented by the feature variance, whereas the strength of features is represented by the activation magnitude. These cues are scaled to the range between 0 and 1 and fed as input to a fuzzy inference system. All the input cues are modeled by linguistic variables, labeled by low, medium, and high with the membership functions corresponding to them respectively. Let μLow(·), μMedium(·), and μHigh(·) denote the membership degrees. Based on these memberships, fuzzy rules are defined to infer feature reliability. Examples of fuzzy rules include: When the feature variance is high and the feature magnitude is low, the inferred reliability is low. This relationship is mathematically expressed as:

$$\mu_r^{\{Low\}} = min\left(\mu_{\{High\}(v^l)}, \mu_{\{Low\}(m^l)}\right) \tag{1}$$

When the feature variance is low and the feature magnitude is high, the inferred reliability is high. This relationship is mathematically expressed as

$$\mu_r^{\{High\}} = min\left(\mu_{\{Low\}(v^l)}, \mu_{\{High\}(m^l)}\right) \tag{2}$$

When both the feature variance and the feature magnitude are at medium levels, the inferred reliability is medium. This relationship is mathematically expressed as

$$\mu_r^{\{Medium\}} = min\left(\mu_{\{Medium\}(v^l)}, \mu_{\{Medium\}(m^l)}\right)) \tag{3}$$

where min(·) denotes the fuzzy AND operator.

The final reliability score is obtained through fuzzy aggregation and defuzzification. Specifically, the reliability value rl ∈ [0, 1] is calculated by applying a weighted average of the inferred linguistic outputs:

$$r^l = \frac{(\sum_k \mu_r^k \cdot c_k)}{(\sum_k \mu_r^k)} \tag{4}$$

where k ∈ {Low, Medium, High} and c_k denotes the corresponding centroid value of each fuzzy set. In the defuzzification stage, the centroid values for the fuzzy reliability sets are defined as cLow = 0.25, cMedium = 0.5, and cHigh = 0.75. These values are chosen as uniformly spaced representative points within the normalized range [0,1], corresponding to low, medium, and high reliability levels. The reliability-weighted encoder feature is then calculated as

$$\{F\}_e^l = r^l \odot F_e^l \tag{5}$$

where ⊙ represents element-wise multiplication. This operation removes the unreliable or noisy features and maintains informative features, and thus the feature fusion on the decoding is stronger.

3.3 Fuzzy Boundary Consistency Module

An accurate definition of lesion borders is essential in COVID-19 segmentation, whereas there is a high rate of uncertainty on the boundaries because of an overlap of intensities and irregularities. To overcome this problem, a fuzzy boundary consistency module is added to the decoder, and it powers up boundary predictions. Let represent the decoder level map feature map at level l obtained during the decoding stage. To take into account the edge information, local gradient magnitude Gl is calculated based on the value of it, whereas regional homogeneity Hl is estimated to express local smoothness. These indications are used as inputs in a different fuzzy inference system. The magnitude of the gradient is defined as a linguistic variable, i.e., the magnitude can be weak, moderate, or strong, and the homogeneity can be low or high. Based on these descriptors, fuzzy inference is employed to estimate boundary confidence. When the gradient magnitude is strong and the local homogeneity is low, the boundary confidence is inferred to be high. This relationship is mathematically expressed as

$$\mu_b^{High} = min\left(\mu_{\{Strong\}}(g^l), \mu_{\{Low\}}(h^l)\right) \quad (6)$$

Conversely, when the gradient magnitude is weak and the homogeneity is high, the boundary confidence is inferred to be low. This relationship is mathematically expressed as

$$\mu_b^{Low} = min\left(\mu_{\{Weak\}}(g^l), \mu_{\{High\}}(h^l)\right) \quad (7)$$

The resulting fuzzy boundary confidence map bl ∈ [0, 1] is used to refine decoder features as follows:

$$\{F\}_d^l = b^l \odot F_d^l + (1 - b^l) \odot F_d^{\{l+1\}} \quad (8)$$

where F_d^{l+1} denotes the decoder feature from the coarser scale. This formula-tion enhances boundary regions while maintaining regional consistency.

3.4 Output Prediction and Loss Function

The refined decoder features are passed using a 1 × 1 convolution layer and sigmoid activation function to produce the final segmentation mask output:

$$Y^{\frown} = \sigma(\text{Conv}_{1\times1}(F^{\frown}_{d1})). \quad (9)$$

To train AFR-Net, a composite loss function is employed, combining region-level accuracy and boundary sensitivity. The final loss is calculated as:

$$L = LDice + \lambda LBCE, \quad (10)$$

where LDice is the dice loss used to handle class imbalance, LBCE is the BCE(Binary Cross Entropy), and λ is a weighting factor balancing the two terms.

The complete training process of AFR-Net is summarized in Algorithm 1. The proposed network is fully trained using backpropagation, and all fuzzy parameters are optimized jointly with network weights. Through the integration of fuzzy feature reliability assessment and boundary consistency reasoning, AFR-Net provides an interpretable and effective framework for uncertainty-aware COVID-19 lesion segmentation.

Algorithm 1 Training Procedure of AFR-Net

Require: Training CT images X, ground truth masks. Y, learning rate η, epochs E

Ensure: Trained network parameters θ

Initialize network parameters θ.
for each = 1 to E do
  for each mini-batch (X,Y) ∈ (X,Y), do
    Extract encoder feature maps using the U-Net encoder.
    for each encoder level l, do
    Compute uncertainty cues (feature variance and activation magnitude).
    Infer fuzzy reliability map RL using fuzzy inference rules.
    Obtain reliability-weighted features.
    end for
      Decode features using skip connections with
      for each decoder level l, do
      Compute gradient magnitude and regional homogeneity.
      Infer fuzzy boundary confidence map
      Refine decoder features using boundary consistency reasoning.
      end for
    Generate segmentation prediction $\hat{Y}$.
    Compute total loss L using Dice and BCE losses.
    Update network parameters θ via backpropagation.
    end for
end for

4. Experiment and Result Analysis

This section describes the dataset used for evaluation, preprocessing steps, implementation details, baseline models, training configuration, and experimental results employed to evaluate the efficiency of the suggested AFR-Net framework.

4.1 Output Prediction and Loss Function

The proposed framework's performance was evaluated on the MosMedData COVID-19 CT dataset [18], which contains 1110 chest CT scans collected from patients with COVID-19-related findings. Each scan includes pixel-level infection annotations provided by expert radiologists. The dataset was separated into three groups, with 70% used for training, 10% for validation, and 20% for testing. Prior to training, each CT slice was rescaled to a fixed spatial resolution to ensure consistency across samples and to fit GPU memory constraints. Intensity values are normalized to the range [0, 1] to reduce inter-scan intensity variations and stabilize network training. To make the model more robust, different data augmentation techniques are applied during training, including random horizontal flips, rotations, and scaling. These operations allow the network to learn useful patterns from a limited dataset and reduce the chance of overfitting. The proposed AFR-Net model is developed using the PyTorch deep learning framework. Its backbone follows a typical U-Net style encoder–decoder structure. The convolution network block contains a 3×3 layer of convolution operation along with batch normalization and a ReLU activation function. The fuzzy feature reliability module and the fuzzy boundary consistency module are added as lightweight components within the network, so they do not noticeably increase the computational complexity. At the time of training, the parameters of the network are optimized with the help of Adam optimization techniques with a starting learning rate of 1×10^{-4}.

Table 1: Performance comparison of COVID-19 lesion segmentation models.

Model	Accuracy (%)	Mean IoU (%)	Dice (%)
U-Net	98.51	73.03	82.71
U-Net++	98.51	73.25	83.75
ResUNet	98.50	72.60	83.23
AFR-Net	**98.52**	**73.80**	**84.16**

When the validation loss plateaus, the learning rate is reduced, and training is performed for 100 epochs, and the model with the best validation performance is selected for final evaluation. All experiments are conducted on a single GPU with sufficient memory to support end-to-end training.

4.2 Baseline Models and Training Protocol

To measure the performance of the proposed AFR-Net, comprehensive comparisons are conducted using several widely adopted deep learning–based segmentation models. Specifically, we consider U-Net, a standard encoder–decoder architecture with skip connections that has become a cornerstone in medical image segmentation [4]. In addition, U-Net++ is included as a stronger baseline due to its nested and dense skip connections, which aim to reduce the semantic gap between encoder and decoder feature maps [5]. Furthermore, ResUNet is employed as a residual learning–based extension of the encoder–decoder paradigm, designed to improve gradient propagation and training stability in deeper networks [17]. All baseline models are implemented under identical

experimental settings for unbiased and fair comparison. All methods utilize the same data splits of training, validation, and testing and have consistent preprocessing, optimizer settings, and loss functions. The models AFR-Net and the baselines are fully trained in a pipeline through a combined loss by merging the two factors, binary cross-entropy loss and dice loss. The formulation of loss is the most effective in terms of dealing with the issue of class imbalance as well as encouraging the delineation of lesion boundaries. The model performance is continuously evaluated on the validation split, and early stopping is employed to mitigate overfitting.

4.3 Result on COVID-19 lesion segmentation dataset

This section presents a comprehensive evaluation of the proposed AFR-Net and compares its performance with widely used baseline segmentation models, namely U-Net, U-Net++, and ResUNet. Both quantitative and qualitative analyses are conducted on a MosMedData COVID-19 CT dataset [18]. The dataset exhibits substantial variability in lesion size, shape, and intensity, with infection regions often showing blurred edges and weak contrast with nearby normal lung tissue, making automated segmentation a challenging task.

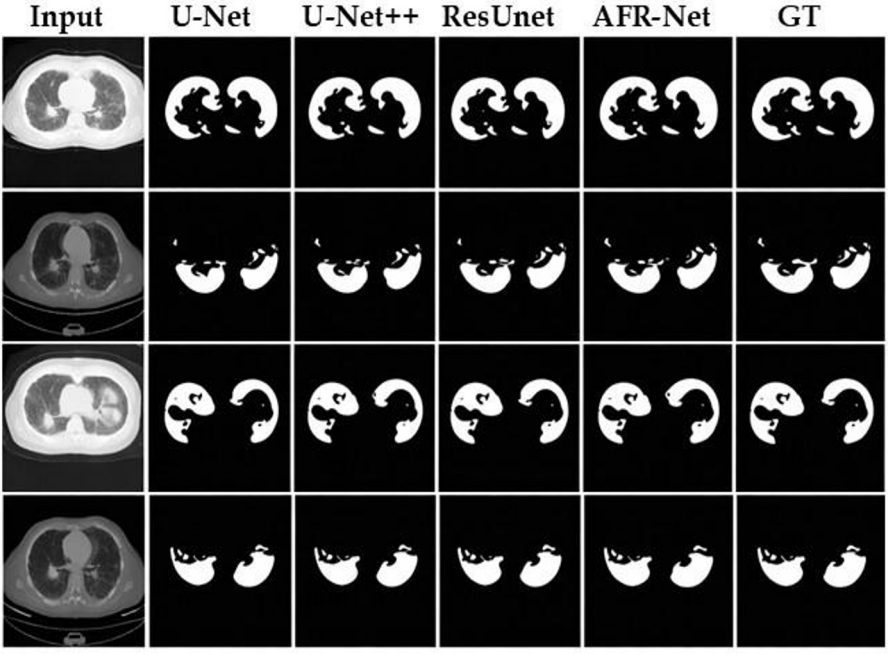

Fig. 2: Visual comparison of segmentation results obtained by different models on the COVID-19 dataset.

Table 1 presents the quantitative performance of all models using three evaluation metrics: accuracy, mean IoU, and Dice coefficient. These metrics are widely used in med-

ical image segmentation to assess segmentation reliability, region overlap, and boundary agreement with ground truth annotations. As observed in Table 1, AFR-Net achieves superior performance compared to competitive baselines across evaluation metrics. Statistical significance was verified using a paired t-test with $p < 0.05$, confirming that the improvements over baseline models are statistically significant. Specifically, it achieves an accuracy of 98.52%, the best mean IoU of 73.80%, and a Dice score of 84.16%, reflecting a better quality of segmentation and consistency of the regions. AFR-Net has a better Dice score and Mean IoU compared to the conventional U-Net variants by about 1.45% and 0.77%, respectively. Consistent gains can also be found compared to U-Net++ and ResUNet, which proves the efficiency of the proposed fuzzy feature reliability and boundary refinement processes. It is important to note that segmentation accuracy may appear high due to the large proportion of background pixels in CT images. Therefore, Dice and Mean IoU are considered more reliable metrics for evaluating lesion segmentation performance.

The qualitative and quantitative comparison of the models based on representative CT slices are presented in Fig. 2 and Fig. 3, respectively. Base U-Net and ResUNet have discontinuous predictions and boundary errors at hard-to-predict zones, and U-Net++ becomes more continuous but continues to make false positives and boundary errors. Conversely, the proposed AFR-Net creates segmentation masks that are much closer to the ground truth, have smoother boundaries, and cover all the lesions. These enhancements are because of the fuzzy feature reliability modeling that inhibits the unreliable features of the encoders and also the fuzzy boundary refinement module that boosts the confidence in the boundary in the decoding process. The

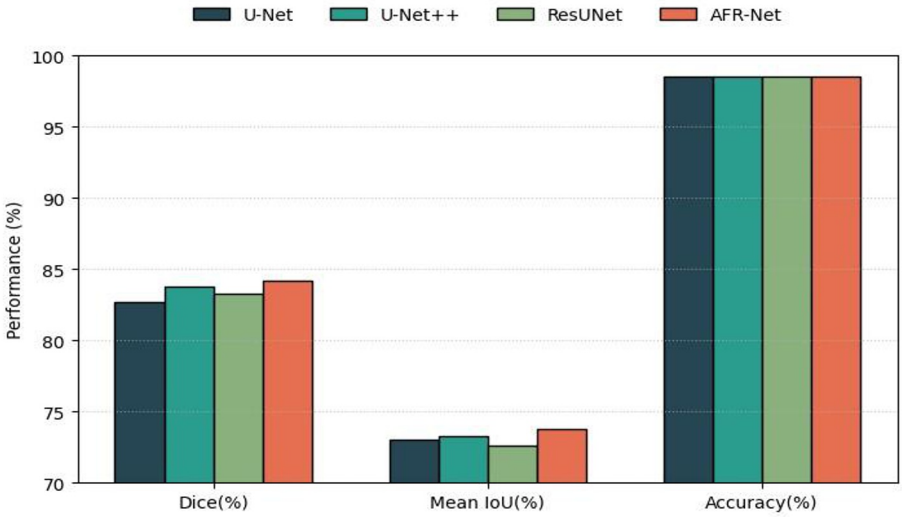

Fig. 3: Quantitative performance comparison of different models on the COVID-19 dataset.

Qualitative observations are strongly supported by the quantitative results in Table 1, where AFR-Net consistently outperforms baseline architectures across all evaluation metrics, demonstrating its effectiveness in detecting COVID-19 lesions in CT images.

5. Conclusion and Future Work

This paper introduced AFR-Net, a fuzzy-based framework of adaptive fuzzy reasoning, which is used to segment lesions in chest CT images of COVID-19. The major issues that the offered approach will resolve include the obscure lesion delimitation and feature ambiguity by integrating the idea of fuzzy features reliability evaluation and fuzzy boundary consistency enhancement into a conventional encoder-decoder setup. The design provides uncertainty modeling and allows it to be architecturally simple at the same time. The experimental findings provide evidence that AFR-Net is more robust than U-Net, U-Net++, and ResUNet in Dice score and mean IoU as well as generates a more coherent and consistent lesion boundary. The effectiveness of the suggested fuzzy reasoning strategy is proven by both quantitative and qualitative analyses carried out to assess the performance of this strategy on ambiguous areas that are typical of COVID-19 CT scans. The future work will include further broadening of the proposed framework into 3D volumetric segmentation and assessing its generalization ability in multicenter data. Moreover, adaptive fuzzy membership learning and the incorporation of clinical priors will also be investigated in order to make it even stronger and more readable. Altogether, the proposed AFR-Net demonstrates promising performance for uncertainty-aware COVID-19 lesion segmentation and may provide useful insights for future research in medical image segmentation.

References

1. Bernheim, A., Mei, X., Huang, M., Yang, Y., Fayad, Z.A., Zhang, N., Diao, K., Lin, B., Zhu, X., Li, K., Li, S., Shan, H.: Chest CT findings in coronavirus disease 19 (COVID-19): Relationship to duration of infection. Radiology 295(3), 685–691 (2020)
2. Fang, Y., Zhang, H., Xie, J., Lin, M., Ying, L., Pang, P., Ji, W.: Sensitivity of chest CT for COVID-19: Comparison to RT-PCR. Radiology 296(2), 115–117 (2020)
3. Shan, H., Gao, Y., Shi, Y., Shi, L., Li, M., Xiong, Z., Yang, Y., Zhang, Y., Zhao, Y., Liang, W.: Lung infection quantification of COVID-19 in CT images with deep learning. IEEE Transactions on Medical Imaging 39(8), 2608–2618 (2020)
4. Ronneberger, O., Fischer, P., Brox, T.: U-Net: Convolutional networks for biomedical image segmentation. In: Navab, N., Hornegger, J., Wells, W.M., Frangi, A.F. (eds.) MICCAI 2015, LNCS, vol. 9351, pp. 234–241. Springer, Cham (2015)
5. Zhou, Z., Siddiquee, M.M.R., Tajbakhsh, N., Liang, J.: UNet++: A nested U-Net architecture for medical image segmentation. In: Stoyanov, D. et al. (eds.) DLMIA 2018, LNCS, vol. 11045, pp. 3–11. Springer, Cham (2018)
6. Abdar, M., Pourpanah, F., Hussain, S., Rezazadegan Tavakoli, M., Liu, L., Ghavamzadeh, M., Khosravi, A., Acharya, U.R., Makarenkov, V., Nahavandi, S.: A review of uncertainty quantification in deep learning: Techniques, applications and challenges. Information Fusion 76, 243–297 (2021)

7. Li, L., Qin, L., Xu, Z., Yin, Y., Wang, X., Kong, B., Bai, J., Lu, Y., Fang, Z., Song, Q.: Automatic COVID-19 lung infection segmentation using deep learning. Artificial Intelligence in Medicine 111, 101990 (2021)
8. Xiao, X., Lian, S., Luo, Z., Li, S.: Weighted Res-UNet for high-quality retina vessel segmentation. In: 9th IEEE International Conference on ITME, pp. 327–331. IEEE, Hangzhou (2018)
9. Oktay, O., Schlemper, J., Folgoc, L., Lee, M., Heinrich, M., Misawa, K., Mori, K., McDonagh, S., Hammerla, N.Y., Kainz, B., Glocker, B., Rueckert, D.: Attention U-Net: Learning where to look for the pancreas. In: Frangi, A.F., et al. (eds.) MICCAI 2018, LNCS, vol. 11071, pp. 447–455. Springer, Cham (2018)
10. Huang, H., Lin, L., Tong, R., Hu, H., Zhang, Q., Iwamoto, Y., Han, X.-H., Chen, Y.-W., Wu, J.: UNet 3+: A full-scale connected U-Net for medical image segmentation. In: ICASSP 2020, pp. 1055–1059. IEEE, Barcelona (2020)
11. Fan, D.-P., Zhou, T., Ji, G.-P., Zhou, Y.-C., Chen, G., Fu, H., Shen, J., Shao, L.: Inf-Net: Automatic COVID-19 lung infection segmentation from CT images. IEEE Transactions on Medical Imaging 39(8), 2626–2637 (2020)
12. Yan, L., Zhang, H., Xiao, Y., Wang, M., Sun, C., Liang, J.: COVID-19 pneumonia diagnosis using a simple 2D deep learning framework with a single chest CT image. Pattern Recognition 110, 107746 (2021)
13. Gal, Y., Ghahramani, Z.: Dropout as a Bayesian approximation: Representing model uncertainty in deep learning. In: ICML 2016, pp. 1050–1059. JMLR.org, New York (2016)
14. Kendall, A., Gal, Y.: What uncertainties do we need in Bayesian deep learning for computer vision? In: Guyon, I., et al. (eds.) NeurIPS 2017, pp. 5574–5584 (2017)
15. Lakshminarayanan, B., Pritzel, A., Blundell, C.: Simple and scalable predictive uncertainty estimation using deep ensembles. In: Guyon, I., et al. (eds.) NeurIPS 2017, pp. 6402–6413 (2017)
16. Zadeh, L.A.: Fuzzy sets. Information and Control 8(3), 338–353 (1965)
17. Zhang, Z., Liu, Q., Wang, Y.: Road extraction by deep residual U-Net. IEEE Geoscience and Remote Sensing Letters 15(5), 749–753 (2018)
18. Morozov, S.P., Andreychenko, A.E., et al.: MosMedData: Chest CT scans with COVID-19 related findings dataset. arXiv preprint arXiv:2005.06465 (2020)